The Permian-Triassic Boundary in the Carnic Alps of Austria (Gartnerkofel Region)			Editors: W.T. Holser & H.P. Schönlaub	
Abh. Geol. B.-A.	ISSN 0378-0864 ISBN 3-900312-74-5	Band **45**	S. 139–148	Wien, Mai 1991

The Permian-Triassic of the Gartnerkofel-1 Core (Carnic Alps, Austria): Sulfur, Organic Carbon and Microspherules

By WILLIAM T. HOLSER*)

With 1 Text-Figure and 3 Plates

Carinthia
Carnic Alps
Permian/Triassic Boundary
Sulfur
Carbon
Microspherules

Österreichische Karte 1 : 50.000
Blatt 198

Contents

Zusammenfassung

Alle mergeligen Zwischenlagen wurden ebenso wie zahlreiche Proben von vorwiegend dolomitischem Kalk des Bohrkernes Gartnerkofel-1 auf organischen Kohlenstoff, pyritischen und geringlöslichen Schwefel untersucht.

Der Gehalt an C_{org} liegt generell unter 0,1 %, obwohl einige der Mergelproben bis auf 0,5 % kommen. Pyritischer Schwefel, allgemein um 0,05 %, ist weit verbreitet, aber zwei Zonen höherer Konzentration sind an negative Abweichungen von $\delta^{13}C$ direkt oberhalb schwacher Iridium-Anomalien gebunden. Framboid-Texturen und $\delta^{34}S$-Gehalte im Pyrit weisen auf einen frühdiagenetischen Ursprung hin.

Bei der Probenaufbereitung auf Conodonten wurden einige Mikrosphären geborgen, die aber als anthropogene Verunreinigungen interpretiert werden.

Abstract

All marly interbeds as well as numerous samples of the dominantly dolomitic limestone core Gartnerkofel-1 were analyzed for organic carbon and pyritic (as well as minor soluble) sulfur.

C_{org} is generally less than 0.1 %, although some of the marls are as high as 0.5 %. Pyritic sulfur, generally in the range 0.05 % is widely distributed, but two zones of higher concentration are associated with negative excursions of $\delta^{13}C$ just above weak iridium anomalies. The framboidal texture and $\delta^{34}S$ levels in the pyrite point to an early diagenetic origin.

A few microspherules were recovered from conodont preparations, but were judged to be man-made contaminants.

1. Introduction

Previous studies have noted that the clay beds associated with the Cretaceous/Tertiary [K/T] boundary contain enhanced levels of pyrite (SCHMITZ, 1988, 1990; SCHMITZ et al., 1988; HANSEN et al., 1986, 1988; JEHANNO, 1987) and organic carbon in the form of kerogen, charcoal and soot (WOLBACH et al., 1985, 1989, 1990; HANSEN et al., 1986, 1987, 1988; SCHMITZ, 1988). Some of the pyrite occurs as microspherules; other microspherules are composed of potassium feldspar (SMIT & KLAVER, 1981; MONTANARI et al., 1983; NASLUND, et al., 1986; IZETT, 1987; JEHANNO et al., 1987; KYTE, 1990), spinel-group minerals (magnetite, spinel, ma-

*) Author's address: Prof. Dr. WILLIAM T. HOLSER, Department of Geological Sciences, University of Oregon, Eugen, OR 97403, USA.

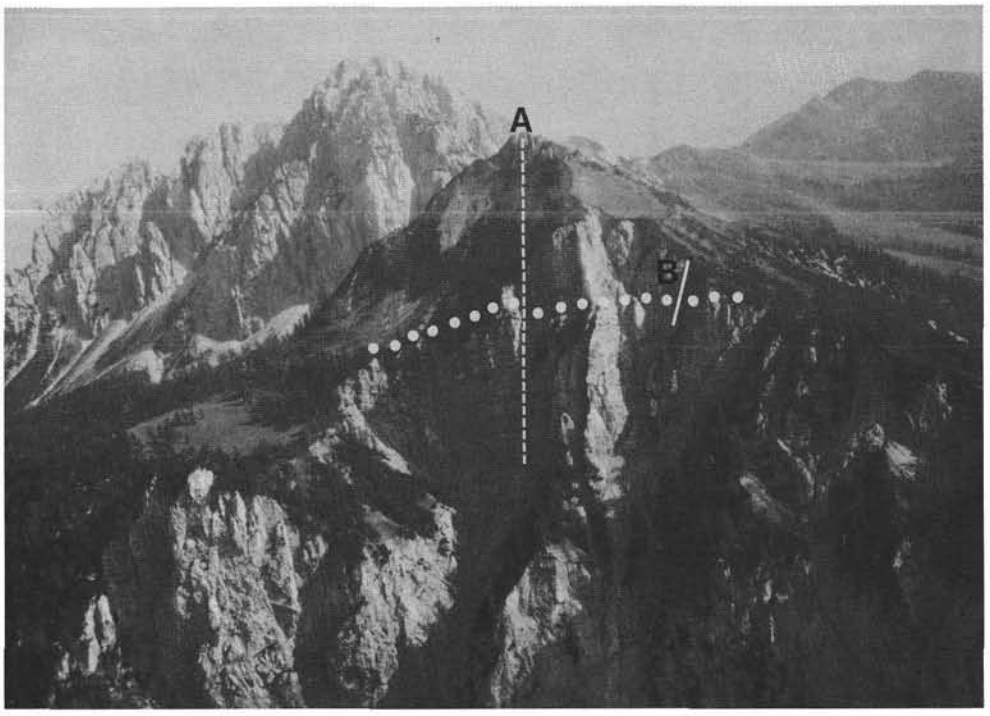

Text-Fig. 1.
Aerial photograph from the north of the Reppwand with the Gartnerkofel (2195 m) in the background.
A: Drill site on Kammleiten (1998 m);
B: Top of the outcrop section.
Dotted line indicates the Permian–Triassic boundary between the Bellerophon Formation (below) and the Werfen Formation above.
Photo: G. FLAJS, Aachen.

gnesioferrite, chromite or ferrite) (MONTANARI et al., 1983; SMIT & KYTE, 1984; KYTE & SMIT, 1986; HANSEN et al., 1986, 1988; IZETT, 1987; JEHANNO et al., 1987; CISOWSKI, 1988), goethite (KYTE & SMIT, 1986; HANSEN et al., 1986: JEHANNO et al., 1987; SCHMITZ, 1988) and other alteration products (kaolinite, glauconite, goyazite, jarosite, apatite) (MONTANARI et al., 1983; KYTE & SMIT, 1986; NASLUND, et al., 1986; BOHOR et al, 1987; IZETT, 1987; JEHANNO et al., 1987; SCHMITZ, 1988; CISOWSKI, 1988). The occurrences of these minerals at the K/T boundary have been emphasized by most of the above authors as important evidence for their respective explanations of the accumulations of iridium and other trace elements and the sequence of events that accompanied then. Consequently it is of interest to compare some related data from the P/Tr boundary at Gartnerkofel with those from the more intensively studied K/T boundary.

2. Chemical Analyses for Sulfur and Carbon

Cuts of all samples were analyzed for total sulfur, total carbon, and for S and C soluble in 2N HCl, in a LECO infrared analyzer, as described by KLEIN (this volume). The results are given in Tables 5, 6 and 7 of KLEIN's paper (this volume).

3. Organic Carbon

The acid treatment obviously dissolved all dolomite and calcite. The acid-insoluble residue of C is designated as "organic carbon", C_{org}, in accordance with traditional laboratory practice. From the point of view of organic geochemistry it includes both kerogen and "elemental carbon", and the latter may include carbon soot as well as coaly components and charcoal (WOLBACH & ANDERS, 1989). The content of C_{org} was very low, less than 0.1 %, even in some of the marly interbeds (prefix "S" in the tables of KLEIN, this volume), which in other cases ranged as high as 0.5 %. Such low levels of C_{org} are probably not suitable for the separation of the components of elemental carbon (WOLBACH & ANDERS, 1989), and these separations have not yet been attempted on P/Tr materials. A suite of samples of the marl/shale interbeds from GK-1 was subjected to standard palynological extraction procedures (with HF), by Dr. R. ZETTER, but failed to recover identifiable spore/pollen materials. A single sample (86450) of marl from the Reppwand outcrop section, in the Bellerophon Formation 4.2 m below the lower Ir-peak, was submitted to J.M. HAYES for a trial analysis of geoporphyrins (HAYES et al, 1989). Soxhlet extraction with organic solvents failed to recover any significant amount of soluble organic material. After most of the contributions to this volume were already in press, new analyses were completed on the carbon isotope ratio of the C_{org} in a selected group of 36 of the marly samples from GK-1 (MAGARITZ et al., submitted). Although rocks with such a low content of C_{org} are not usually studied by isotope analysis, the results were very consistent and make an interesting and critical complement to the isotope studies of the carbonate fraction described here by MAGARITZ & HOLSER (this volume). One important conclusion is that the C_{org} in the interbeds of the core material is substantially unaltered by weathering.

4. Pyrite

The significant sulfur determination is total sulfur, S_{tot}. Sulfur soluble in the 2N HCl etch, S_{sol}, is calculated by difference, $S_{tot}-S_{ins}$, and with the precision of individual sulfur analyses as low as 10 %, the soluble differences are probably not significant unless they amount to over 15 % of S_{tot}. It also seems likely that

the precision may be even worse where $S_{tot} < 0.1$ %. Only five samples (S101, S117, S118B, S190 and S193) had $S_{sol} > 0.1$ % (KLEIN, this volume). In one of these (S118B) FENNINGER (this volume) found 4 % gypsum by X-ray diffraction, and it seems likely that the S_{sol} in the other four samples, as well as in many of those showing lower levels of S_{sol}, is also accounted for by HCl-soluble sulfate in gypsum. Two of the samples with high S_{sol} showed equal and low sulfur isotope ratios in soluble and insoluble fractions (PAK & HOLSER, this volume). This indicates that the sulfate is not primary as sulfate, but was a product of recent oxidation of (insoluble) sulfide, either by oxidizing ground waters or by air exposure after coring. A minor amount of the sulfate formed in this way may have been lost from the rock through solution in ground water. We cannot firmly preclude the presence, in some of the five samples, of minor amounts of the mineral pyrrhotite, FeS, which is soluble in HCl, but examination by polarized reflection microscopy of a polished slab of core from next to sample S117 showed only pyrite and no pyrrhotite. Consequently for our interest in primary and diagenetic geochemistry, S_{tot} represents S as pyrite; in the few samples with high S_{sol} it may slightly underestimate the original amount of pyrite.

The data for S_{tot} in the GK-1 core (KLEIN, this volume) reveal a wide distribution of minor amounts of pyrite, at levels generally in the range of 0.05 % pyrite. Two zones of higher concentration of 1–10 % pyrite are evident at 185.5–186.5 and 215.1–222.2 m, in each case just above the narrow intervals of shaly material (at 186.6 and 224.5 m) that show moderate peaks of Ir and other trace metals: compare the plots of S and Ir/Al in Text-Fig. 10 of HOLSER et al. (this volume). Sample S117, at 185.5 m, just above the upper Ir peak and 45 m above the P/Tr stratigraphic boundary, was particularly rich in pyrite, analyzing 12.6 % S (KLEIN, this volume) and 27 % Fe (ATTREP et al., this volume). This material was studied in detail by transmitted and reflected light microscopy, and by electron microprobe.

The main concentration of pyrite comprises a 2-cm thick sequence of wavy mm lamellae of pyrite, with lenses of dolomite or open space. The proportion of dolomite increases and its grain size decreases upward, but at least a few grains of cubic or microspheroidal pyrite are disseminated in the beds above. Textures of the pyrite are illustrated in the photomicrographs of Plate 1. Fig. 1 shows the lamellar and disseminated texture of fine-grained pyrite common in the upper part of the bed. In Fig. 2 both framboidal microspherules and small atoll aggregates are evident. The atoll microspherules are larger and more clearly defined in Figs. 4 and 5. Stylolites are generally crosscutting to the pyrite textures, as clearly demonstrated in Fig. 6 where two atoll aggregates have been beheaded by a stylolite. Framboidal microspheres of pyrite are common in modern marine muds (as greigite or other precursor of pyrite), in ancient shales and especially in stratabound sulfide ore deposits (LOVE & AMSTUTZ, 1966; RAMDOHR, 1960). In such occurrences its early diagenetic origin is generally recognized.

Pyrite in its variety of textures was analyzed for trace elements by electron microprobe. Cobalt was consistently detected at a level of 1000 ± 90 ppm ($n = 14$). Other trace elements were not detected, at the sensitivities indicated: As (<500 ppm), Cu (<400 ppm), Mn (<400 ppm), Ni (<500 ppm), Sb (<3000 ppm). Aggregates of pyrite in solid microspherules, atoll texture and single cubes showed no evidence of concentric zoning in Co content. Pyrite forms solid solutions with Co, Ni, and As, and traces of these elements are not unusual in the pyrite of ore deposits (e.g., EWERS & HUDSON, 1972; OSTWALD & ENGLAND, 1979). The lack of variation in trace element content of the GK-1 pyrite, both within and among crystals, is consistent with a uniformity of origin.

Alteration of the pyrite to goethite and hematite is common in GK-1, in some places dominant. Millimolar concentrations of Fe generally exceed those of S_2, as shown in Text-Fig. 10 of Holser et al. (this volume), depending on the amount of alteration. Much of the goethite and hematite has reversed polarity chemical remanent magnetization, of a direction consistent with oxidation of the pyrite during the Cretaceous reversed interval (ZEISSL & MAURITSCH, this volume). Neither S as analyzed, nor Fe as representative of the amount of S present before alteration, has a consistent correlation with C_{org}, as found in many modern sediments and ancient shales (ANDERSON et al, 1987; BERNER & RAISWELL, 1983). Nevertheless, the textures and the sulfur isotope relations (PAK & HOLSER, this volume) strongly indicate early diagenetic deposition of the pyrite.

5. Microspherules

In view of the prominent occurrence of microspherules of various compositions in the K/T boundary clay, and their importance in the interpretation of that bed as fallout from an impact or volcanic event (see references in introduction to this paper), a concerted search as made for any microspherules in the Gartnerkofel P/Tr section. Thin sections, polished sections and oil-immersion samples of the marly interbeds of both the GK-1 core and the outcrop section, especially those with enhanced levels of Ir and other trace elements, were scanned by microscopy, and fracture surfaces were studied by scanning electron microscopy. No microspherules were found in these whole-rock preparations, except for the pyrite (and oxidized pyrite) microspherules described above.

However, in the course of examining acid-insoluble residues of samples from the outcrop section for conodonts, SCHÖNLAUB (this volume) separated five microspherules. Each single example turned up in a residue from solution in acetic acid of a large (0.7 to 2 kg) sample of dolostone. The result was unexpected, and no particular precautions had been taken to minimize contamination from atmospheric fallout on the outcrop or in the laboratory.

Examined under a binocular microscope, the microspherules appeared nearly perfectly spherical. Four were shiny black and from 50 to 150 μm in diameter; the other was matte white and about 250 μm in diameter. They were studied further by SEM; then they were ground to about mid-section and polished for study by vertical optical illumination and electron microprobe. In the sectioning process one of the four black microspherules was lost.

The black microspherules display a beautful dendritic texture, with branching conforming closely to the spherical surface (Pl. 2, Figs. 1–3). Evidently an origi-

nally spherical mass crystallized (or re-crystallized) into a single dendritic crystal – or perhaps several subparallel crystals. Plate 2, Fig. 2 displays 4–fold symmetry around an axis in the upper right. One of the black spherules showed up as a hollow shell on sectioning (Pl. 2, Figs. 4,5), but the other two were solid at the level sectioned (Pl. 2, Fig. 6).

Six microprobe analyses of two spots on each of three black microspherules were very similar, with mean values FeO 89.6 ± 1.9, MnO 0.7 ± 0.3, Cr_2O_3 0.13 ± 0.07 wt %, and with NiO and CoO undetected at <0.10 and <0.23 %, respectively. Two black spherules were also analyzed for other elements using a silicate standard. Although this standard was inappropriate for this mainly iron oxide composition, the detection of BaO at 0.17 ± 0.04 and Al_2O_3 at 0.12 ± 0.05 % may be qualitatively significant in view of fact that these two elements are the principal constituents of the white microspherule (see below).

The mean of the iron analyses, equivalent to 69.7 ± 1.5 wt % Fe, corresponds closely to the ideal composition of Fe_2O_3, 69.94 % Fe. The phase could be either hematite or maghemite, but the 4–fold symmetry of the dendritic texture, and a lack of optical anisotropy in polished section, indicates that cubic maghemite is more likely. Maghemite is usually a metastable oxidation alteration of magnetite, and the crystal form we are seeing in Plate 2 may indeed be simply pseudomorphic after an initial crystallization as magnetite.

In Plate 3, Figs. 1 and 2, the surface of the white microspherule displays a texture of crystallinity that is superficially similar to that of the black microspherules. On closer examina tion (Pl. 3, Fig. 2), and especially in polished section (Pl. 3, Fig. 3), the crystal form is seen to be a radial-acicular texture of elongate crystals.

Microprobe analysis (n = 5) of the white microspherule gives as main constituents only BaO and Al_2O_3, whose mole ratio $Ba/(Ba + Al) = 0.0760 \pm 0.0045$ corresponds rather well to an ideal for $BaO : 6Al_2O_3$ of 0.0769. The analysis also shows traces of a few tenths percent of Ca, Si and Sr. $Ba : 6Al_2O_3$ has not been found in nature, but is found in the synthetic system $BaO - Al_2O_3$, melting congruently at 1915°C (LEVIN, et al., 1964, Fig. 206). Its minimum eutectic melting point in this binary system is 1620°C, at 38 wt % BaO. Neither neighboring phase in the binary system, Al_2O_3 nor $BaO : Al_2O_3$, was evident in the material analyzed. $BaO : 6Al_2O_3$ is probably isostructural with the well-known synthetic compound barium ferrite, a layer stacking of hematite and BaO units.

The uniqueness, purity and extremely high melting point of this material strongly indicates that it is a contaminant from atmospheric fallout during collection or processing of the natural sample. Microspherules routinely encountered in atmospheric fallout are magnetite from welding sputter, Bessemer converter operation, or fly ash from coal-fired electrical generating plants or trash incinerators (McCRONE & DELLY, 1973). In the last decade, however, there has been a great increase in microparticulate debris from space craft, most of it rich in alumina (ZOLENSKY et al., 1989). The main sources of this material are solid rocket fuel exhaust, solid rocket motor ablation, and thermal reflective spacecraft paint. According to ZOLENSKY et al. (1989) the most commonly used paint is composed of micron-sized particles of alumina, titania, and ZnO, but the equally high melting points of compounds in the system Al_2O_3 suggests that such material might also be applied to spacecraft surfaces, and subsequently contribute to particulate atmospheric fallout.

Black iron oxide spherules similar to those described above from Gartnerkofel samples have a wide range of both natural and anthropogenic origins. Black iron oxide microspherules, including hollow structures, associated with the Permian-Triassic boundary in South China, have been variously ascribed to an origin from ablation of an impacting meteorite (GAO et al., 1989), volcanism (ZHANG et al., 1989) or mineralization of algal remains (HANSEN et al, 1989). But the possible detection of traces of Ba in those from Gartnerkofel suggests an unusual common, and therefore man-made, source for all of our microspherules, black and white. It does not seem useful to speculate further on the origin of the black microspherules, pending further collections of material, carefully controlled to minimize contamination.

6. Conclusions

Sulfide is concentrated in narrow zones of pyrite (oxidized in part) above trace metal peaks in the Gartnerkofel section. Its form as lamina composed mainly of framboidal microspherules, intersected by stylolites, and its light sulfur isotope ratio, indicate deposition of the pyrite during early diagenesis. The moderate concentrations of Ir, Co, and Ni in the underlying bed were probably formed in a related reduction process, as postulated by SCHMITZ (1985) for the marine K/T boundary. Organic carbon is relatively low in concentration (a few tenths percent), relative to C/S ratios commonly encountered in marine rocks, but its isotope profile verifies a primary origin. A few microspherules picked from conodont preparations are likely a contaminant from atmospheric fallout.

Acknowledgements

I thank Michael SCHAFFER for expert assistance in SEM and electron microprobe analysis, Donald BROWNLEE for preparation of the polished sections of microspherules, and Harry HOWARD for photomicrographs.

Plate 1

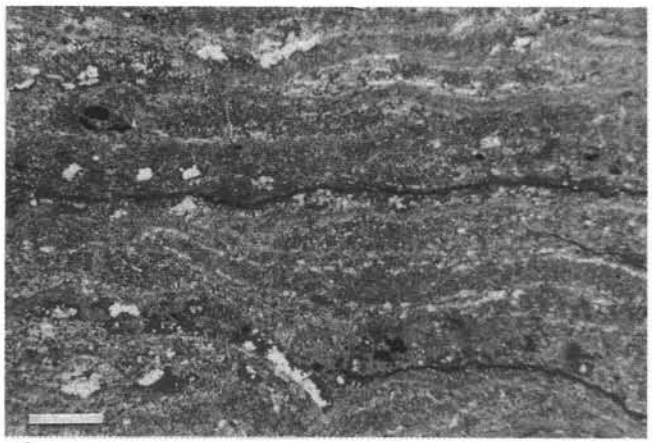

1

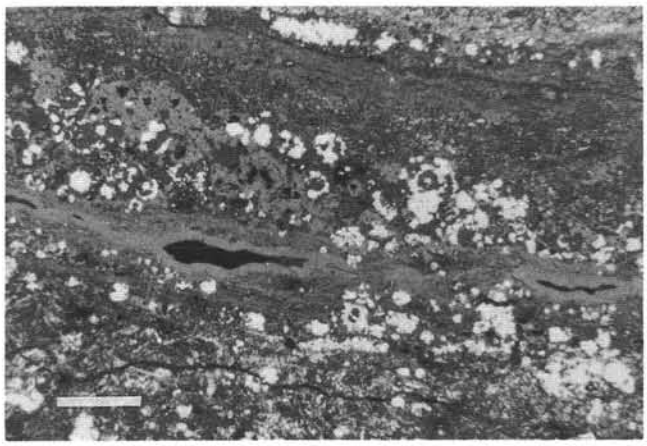

2

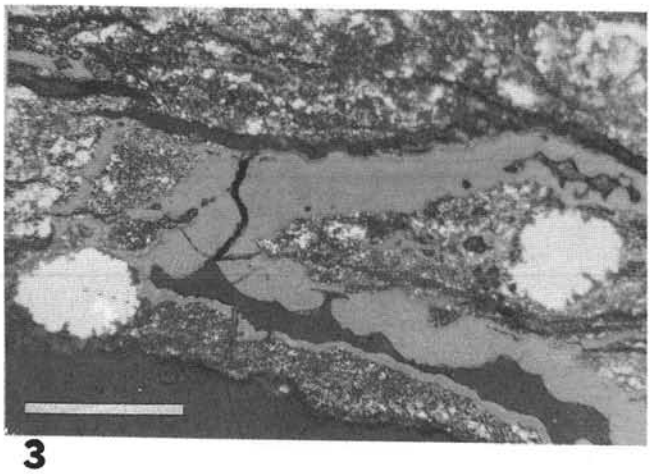

3

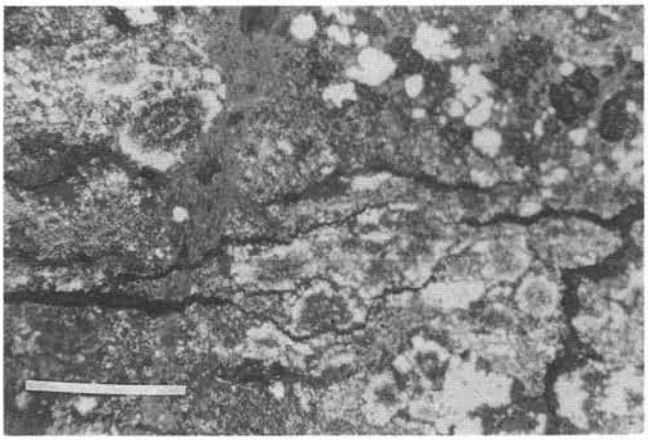

4

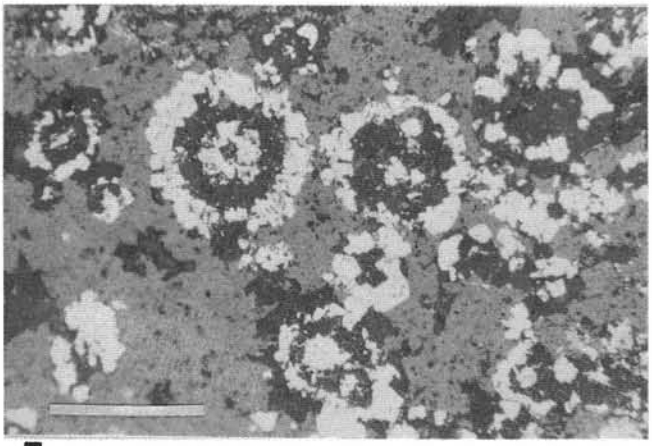

5

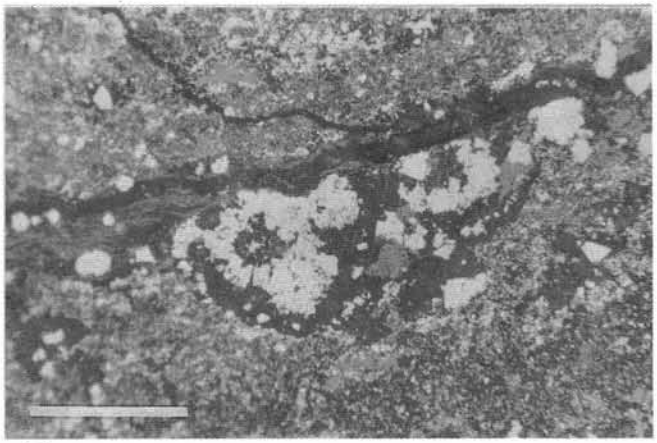

6

Photomicrographs in reflected light of textures in the pyrite bed at 185.55 m.

Fig. 1: Fine-grained pyrite in wavy-lamellar and disseminated texture; a few grains are cubic.
Fig. 2: Framboidal microspherules of pyrite, some with atoll texture.
Fig. 3: Microspherules of pyrite, with later stylolites.
Fig. 4: Sieve-textured aggregates and microspherules of pyrite.
Fig. 5: Well-developed atoll texture in pyrite.
Fig. 6: Atoll microspherules of pyrite intersected by later stylolite.

White: pyrite; light gray: hematite and goethite; dark gray: quartz; black: open space, or clay-rich stylolite.
Scale bars: 100 μm.

Plate 2

Images of black iron oxide microspherules.

Fig. 1: SEM image, illustrating dendritic single(?)-crystal of maghemite, with branching conforming to the spheroidal shape of the grain.
Scale bar 100 μm.

Fig. 2: Magnified view of the same spherule as in Fig. 1.
Scale bar 100 μm.

Fig. 3: Further magnification of spherule surface, showing detail of crystallographic parallel dendrite branches.
Scale bar 10 μm.

Fig. 4: Photomicrograph by vertical illumination of a polished mid-section of the same spherule, showing hollow structure and crystallinity.
Scale bar 100 μm.

Fig. 5: Same as (D), at higher magnification.
Scale bar = 100 μm.

Fig. 6: Another black iron oxide spherule with no hollow center, but crystallinity similar to Fig. 1.
Scale bar 100 μm.

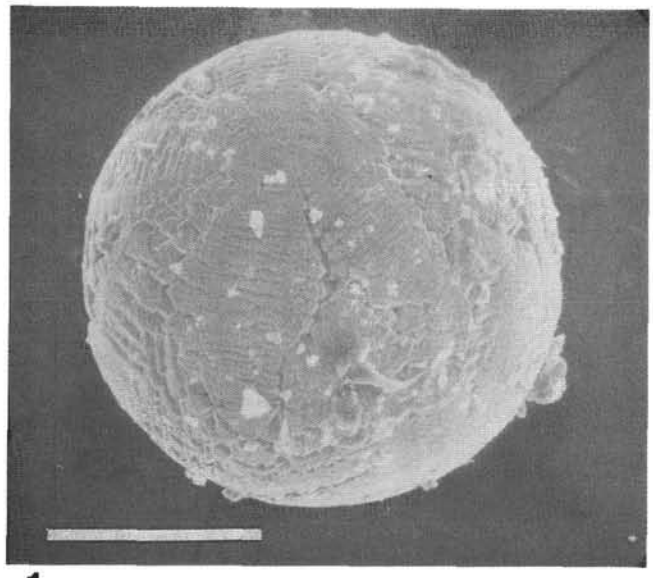

1

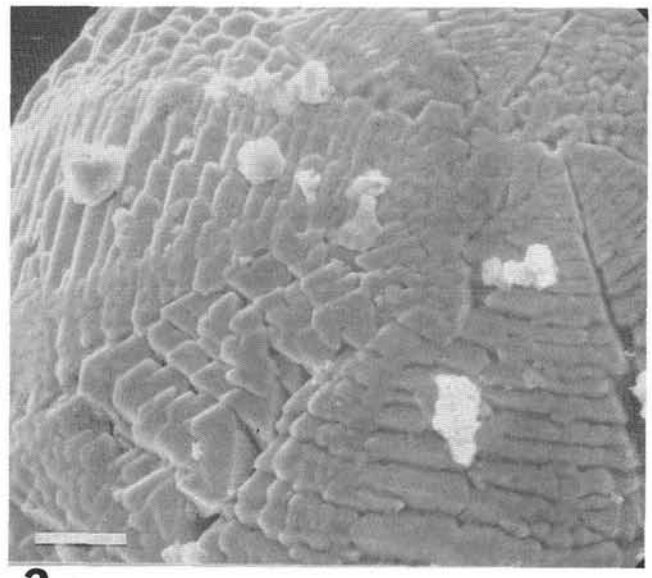

2

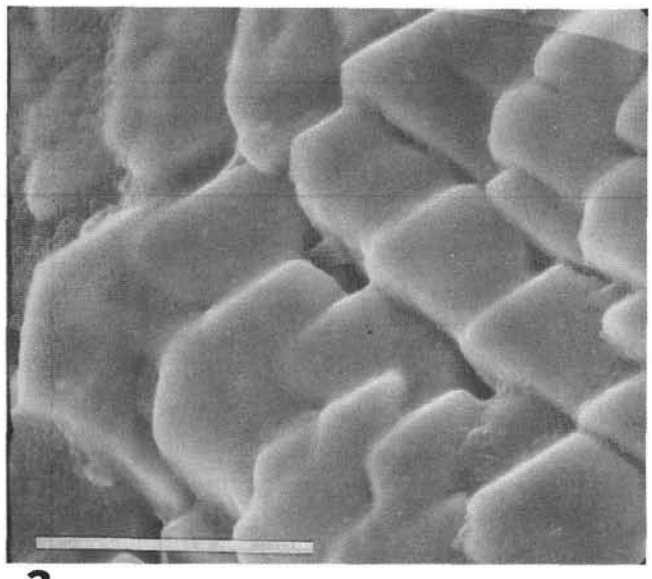

3

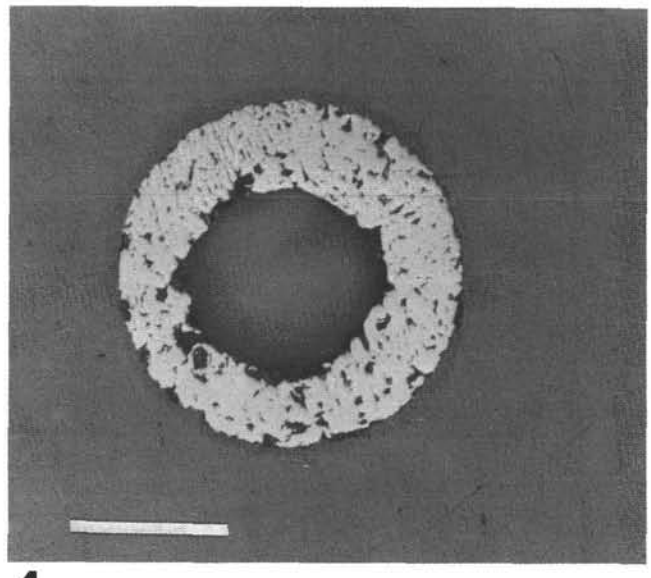

4

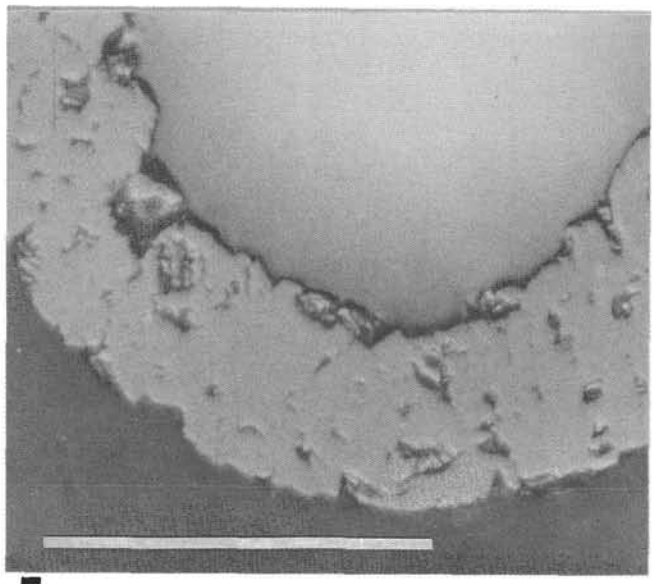

5

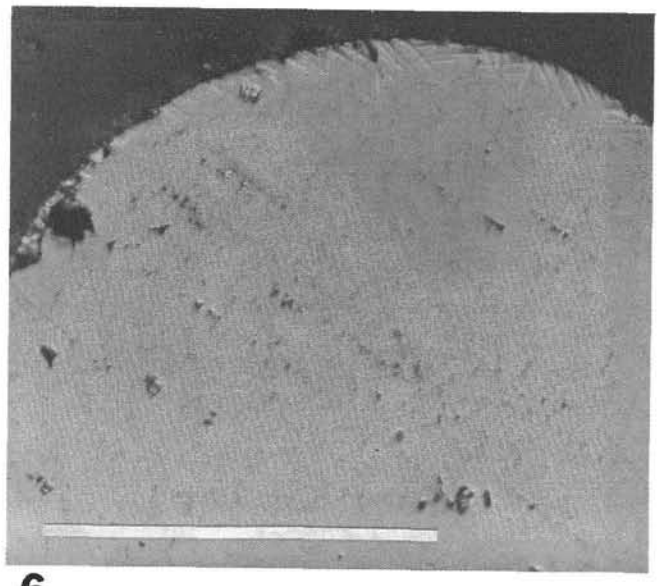

6

Plate 3

Images of white barium aluminate microspherule.

Fig. 1: SEM view of spherule, with surface crystallinity superficially similar to the iron oxide spherules in Plate 2. However, the texture of the surface reflects a randomly oriented acicular crystallinity, compared with the regular orientation of the dendritic branching of the black spherules.
Scale bar 100 μm.

Fig. 2: Acicular intergrowths evident on a closer examination of the surface.
Scale bar 10 μm.

Fig. 3: Polished mid-section of the white spherule, showing the radiating to randomly oriented crystal needles of barium aluminate.
Scale bar 100 μm.

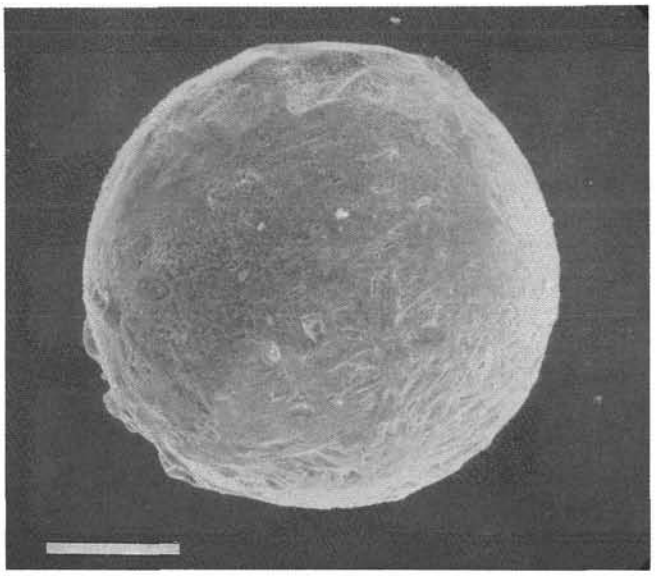

1

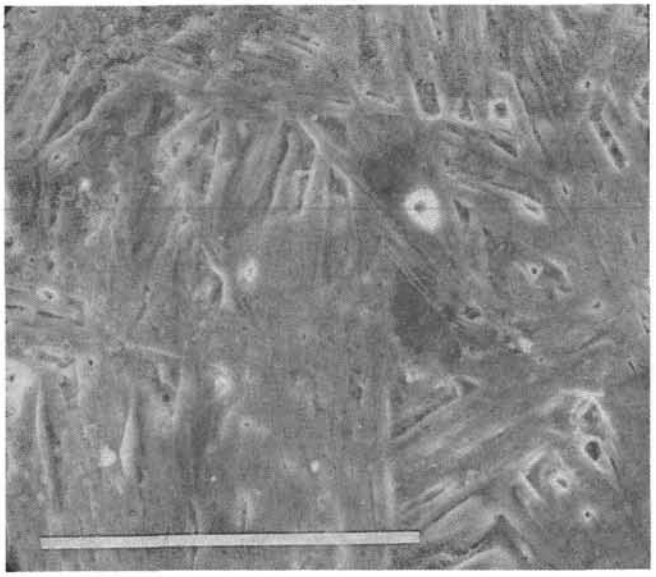

2

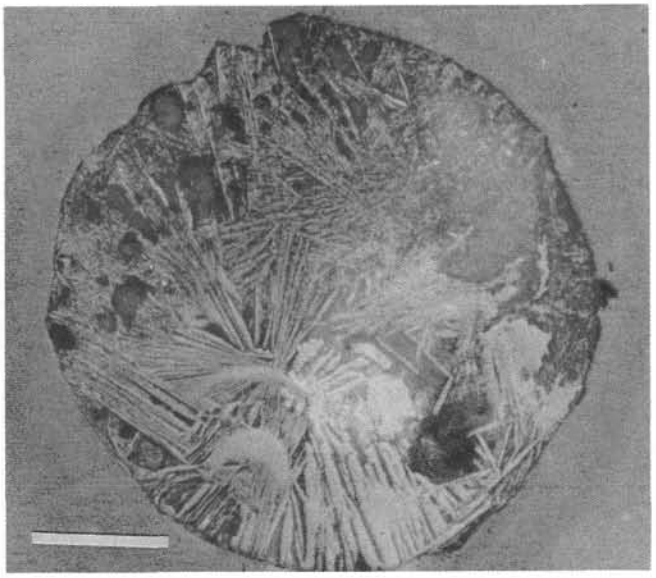

3

References

ANDERSON, T.F., KRUGER, J. & RAISWELL, R.: C-S-Fe Relationships and the Isotopic Composition of Pyrite in the New Albany Shale of the Illinois Basin, U.S.A. – Geochim. Cosmochim. Acta, **51**, 2795–2805, New York 1987.

BERNER, R.A. & RAISWELL, R.: Burial of Organic Carbon and Pyrite Sulfur in Sediments over Phanerozoic Time: A new theory. – Geochim. Cosmochim. Acta, **47**, 835–862, New York 1983.

BOHOR, B.F., TRIPLEHORN, D.M., NICHOLS, D.J. & MILLARD, H.T., Jr.: Dinosaurs, Spherules, and the "Magic" Layer: A New K-T Boundary Clay Site in Wyoming. – Geology, **15**, 896–899, Boulder 1987.

CISOWSKI, S.M.: Magnetic Properties of K/T and E/O Microspheres: Origin by Combustion? – Earth Planet. Sci. Lett., **88**, 193–208, Amsterdam 1988.

EWERS, W.E. & HUDSON D.R.: An Interpretative Study of Nickel-Iron Sulfide Ore Intersection, Lunnon Shoot, Kamblada, Western Australia. – Econ. Geol., **67** 1075–1082.

GAO Z.-G., XU D.-Y., ZHANG Q.-W.& SUN Y.-Y.: Microspherules at the Permian-Triassic Boundary, Shangsi Section, Sichuan, China. – Paper presented at IGCP 199 Meeting, Beijing 1989.

HANSEN, H.J., GWOZDZ, R., BROMLEY, R.G., RASMUSSEN, K.L., VOEGENSEN, E.W. & PEDERSEN, K.R. : Cretaceous-Tertiary Boundary Spherules from Denmark, New Zealand and Spain. – Bull. Geol. Soc. Denmark, **35**, 75–82, Copenhagen 1986.

HANSEN, H.J., GWOZDZ, R. & RASMUSSEN, K.L.: High-Resolution Trace Element Chemistry Across the Cretaceous-Tertiary Boundary in Denmark. – Rev. Españ. Paleontol., No. Extraordinario, p. 21– 29, Madrid 1988.

HANSEN, H.J., RASMUSSEN, K.L., GWOZDZ, R. & KUNZENDORF, H.: Iridium-Bearing Carbon Black at the Cretaceous-Tertiary Boundary. – Bull. Geol. Soc. Denmark, **36**, 305–314, Copenhagen 1987.

HANSEN, H.J., YIN H. & VOGENSEN, E.: The Spherules at the Chinese Permo-Triassic Boundary of Terrestrial Origin. – IGCP 199 Meeting, Beijing, Abstr. p. 8, Beijing 1989.

HAYES, J.M., POPP, B.N., TAKIGIKU, R. & JOHNSON, M. W.: An Isotopic Study of Biogeochemical Relationships between Carbonates and Organic Carbon in the Greenhorn Formation. – Geochim. Cosmochim. Acta, **53**, 2961–2972, New York 1989.

IZETT, G.A.: Authigenic "Spherules" in K-T Boundary Sediments at Caravaca, Spain, and Raton Basin, Colorado and New Mexico, May not be Impact Derived. – Geol. Soc. Amer. Bull., **99**, 78–86, Boulder 1987.

JEHANNO, C. BOCLET, D., BONTE, P., DEVINEAU, J. & ROCCHIA, R.: *L'iridium dans les minéraux a la limite Crétacé–Tertiare* de plusieurs sites européens et africains. – Mém. Soc. Géol. France, **150**, 81–94, Paris 1987.

KYTE, F.T.: Comment on "Origin of Microlayering in Worldwide Distributed Ir-rich Marine Cretaceous/Tertiary Boundary Clays". – Geology, **18**, 87–88, Boulder 1990.

KYTE, F.T. & SMIT, J.: Regional Variations in Spinel Composition: An Important Key to the Cretaceous/Tertiary Event. – Geology, **14**, 485–487, Boulder 1986.

LEVIN, E.M., ROBBINS, D.R. & MCMURDIE, H.F.: Phase Diagrams for Ceramists. – American Ceramic Society, Columbus 1964.

LOVE, L.G. & AMSTUTZ, G.C.: Review of Microscopic Pyrite. – Fortschr. Mineral., **43**, 273–309, Stuttgart 1966.

MAGARITZ, M., KRISHNAMURTHY, R.V. & HOLSER, W.T.: On the Parallel Trends in Carbon Isotopes of Organic and Inorganic Carbon Reservoirs Across the Permian/Triassic Boundary. – Nature (submitted), London.

MCCRONE, W.C. & DELLY, J.G.: The Particle Atlas, 2nd ed, v. 3, Ann Arbor (Ann Arbor Scientific Publishing) 1973.

MONTANARI, A., HAY, R.L., ALVAREZ, W., ASARO, F., MICHEL, H.V. & ALVAREZ, L.W.: Spheroids at the Cretaceous-Tertiary Boundary are Altered Impact Droplets of Basaltic Composition. – Geology, **11**, 668–671, Boulder 1983.

NASLUND, H.R., OFFICER, C.B. & JOHNSON, G.D.: Micro-Spherules in Upper Cretaceous and Lower Tertiary Clay Layers at Gubbio, Italy. – Geology, **14**, 923–926, Boulder 1986.

OSTWALD, J.& ENGLAND, B.M.: The Relationship between Euhedral and Framboidal Pyrite in Base-Metal Sulphide Ores. – Mineral. Mag., **43**, 297–300, London 1979.

RAMDOHR, P.: Die Erzmineralien und ihre Verwachsungen. – 3. Aufl., Berlin (Akademie-Verlag) 1960.

SCHMITZ, B.: Metal Precipitation in the Cretaceous-Tertiary Boundary Clay at Stevns Klint, Denmark. – Geochim. Cosmochim. Acta, **49**, 2361–2370, New York 1985.

SCHMITZ, B.: Origin of Microlayering in Worldwide Distributed Ir-rich Marine Cretaceous/Tertiary Boundary Clays. – Geology, **16**, 1068–1072, Boulder 1988.

SCHMITZ, B.: Reply to Comments on "Origin of Microlayering in Worldwide Distributed Ir-rich Marine Cretaceous/Tertiary Boundary Clays". – Geology, **18**, 87–94, Boulder 1990.

SMIT, J. & KYTE, F.T.: Siderophile-Rich Magnetic Spheroids from the Cretaceous-Tertiary Boundary in Umbria, Italy. – Nature, **310**, 403–405 1984.

SMIT, J. & KLAVER, G.: Sanidine Spherules at the Cretaceous-Tertiary Boundary Indicate a Large Impact Event. – Nature, **292**, 47–49, London 1981.

WOLBACH, W.S., ANDERS, E. & NAZAROV, M. A.: Fires at the K/T Boundary: Carbon at the Sumbar, Turkmenia, Site. – Geochim. Cosmochim. Acta, **54**, 1133–1146, New York 1990.

WOLBACH, W.D., GILMOUR, I., ANDERS, E., ORTH, C.J. & BROOKS, R. R.: Global Fire at the Cretaceous-Tertiary Boundary. – Nature, **334**, 665–669, London 1988.

WOLBACH, W.S., LEWIS, R.S. & ANDERS, E.: Cretaceous Extinctions: *Evidence for Wildfires and Search for Meteoritic* Material. – Science, **230**, 167–170, Washington 1985.

ZHANG K. & YANG S.: Preliminary Study of Microspherules from Permian-Triassic Boundary in South China. – IGCP 199 Meeting, Beijing, Abstr., p. 35, Beijing 1989.

ZOLENSKY, M.E., MCKAY, D.S. & KACZOR, L.A.: A Ten-Fold Increase in the Abundance of Large Solid Particles in the Stratosphere, as Measured for the Period 1976–1984. – J. Geophys. Res., **94D**, 1047–1056, Washington 1989.